

Accepted Manuscript

Title: Nozzle arrangement effect on cooling performance of saline water spray cooling

Author: M.H. Sadafi, Ingo Jahn, Kamel Hooman

PII: S1359-4311(16)30028-X

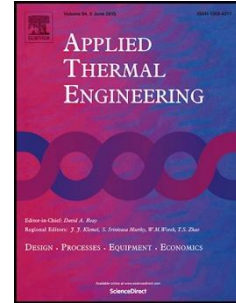
DOI: <http://dx.doi.org/doi: 10.1016/j.applthermaleng.2016.01.078>

Reference: ATE 7638

To appear in: *Applied Thermal Engineering*

Received date: 21-11-2015

Accepted date: 20-1-2016



Please cite this article as: M.H. Sadafi, Ingo Jahn, Kamel Hooman, Nozzle arrangement effect on cooling performance of saline water spray cooling, *Applied Thermal Engineering* (2016), <http://dx.doi.org/doi: 10.1016/j.applthermaleng.2016.01.078>.

This is a PDF file of an unedited manuscript that has been accepted for publication. As a service to our customers we are providing this early version of the manuscript. The manuscript will undergo copyediting, typesetting, and review of the resulting proof before it is published in its final form. Please note that during the production process errors may be discovered which could affect the content, and all legal disclaimers that apply to the journal pertain.

Nozzle Arrangement Effect on Cooling Performance of Saline Water Spray Cooling

M.H. Sadafi^{*}, Ingo Jahn, Kamel Hooman

School of Mechanical and Mining Engineering, The University of Queensland, QLD 4072, Australia

Highlights

- Nozzle arrangements providing more uniform cooled area achieve an improved performance.
- Efficient nozzle arrangement may improve the cooling efficiency of natural draft cooling towers by 2.9%.
- For all arrangements in this study, a dry stream forms before 2.26 m from the nozzles.
- The nozzle arrangement does not influence the wet length significantly.

ABSTRACT: Hybrid cooling is a promising technology to improve the performance of natural draft dry cooling towers. This article presents a computational fluid dynamics study analysing the use of saline water in a spray assisted natural draft dry cooling tower. A multicomponent Discrete Phase Model in ANSYS FLUENT is modified, using the porosity and final shape of dried crystals, and applied for the simulation of solid containing droplets in a spray. To investigate the influence of nozzle arrangements on cooling performance of the sprays, a group of arrangements using six cone nozzles are considered, and the most efficient arrangement is presented. This paper provides new fundamental understanding in the area of saline spray cooling, and shows that nozzle arrangement may improve the cooling efficiency by 2.9%.

Keywords: saline water; hybrid cooling; discrete phase model; multicomponent; heat and mass transfer; nozzle arrangement.

1. Introduction

In a power plant cooling towers exhaust heat to the ambient. Improvements of cooling tower performance lead to increases of a power plant thermal efficiency. To enhance the performance of a natural draft dry cooling tower, hybrid cooling methods are suggested [1, 2]. The two most common methods include water deluge and evaporative cooling, the latter is more efficient due to a higher heat and mass transfer contact area. Moreover, hybrid cooling uses less water compared to water deluge. In evaporative cooling, water spray cools down the inlet air (Fig 1), which leads to drop of minimum temperature of the thermodynamic cycle and consequently, increase of a power plant thermal (power conversion) efficiency. That is, compared to an identical dry cooling plant, more power can be generated using the same amount of heat input when spray cooling is used.

Nonetheless, due to scarcity of natural water resources in hot arid areas, using saline water for spray assisted dry cooling towers is suggested as a promising alternative.

* Corresponding Author. Tel: +61 7 3365 1661. E-Mail addresses: m.sadafi@uq.edu.au (or mhsadafi@gmail.com), i.jahn@uq.edu.au, k.hooman@uq.edu.au

Sadafi et al. developed a CFD model to simulate a single cone spray using saline water [3] in a vertical cooling tower representative arrangement. By comparing the results obtained for 3% NaCl concentration (by mass) with pure water, they showed that using saline water shortens the length from the nozzle, covered by the wet stream. This is a notable benefit, as it allows designers to reduce the distance between the nozzle and the heat exchangers, thereby shortening cooling towers without loss of spray cooling efficiency. In a subsequent study, Sadafi et al. verified their CFD model against their experimental results obtained from a Phase Doppler Interferometry (PDI) study. They showed that in a spray, large droplets push the smaller ones to the middle of the flow [4]. Considering the design parameters (those which can be changed by the designer), the authors presented two dimensionless correlations to predict the wet length and cooling efficiency of a full cone nozzle.

However, due to existence of metal surfaces, the corrosion of heat exchangers and deposition of salt are the pitfalls of using saline water to pre-cool the air in a cooling tower. These drawbacks can be avoided by a proper engineering design. For example, corrosion-resistive materials can be used. Condamine power station in Australia uses a titanium condenser and fibreglass transmitting pipelines to avoid the above-mentioned issues. Other engineering methods include: painting and surface treatments [5, 6], limiting water temperature [6, 7] and cathodic protection [8].

Despite its profound effect on the tower cooling efficiency, arrangement of nozzles in a cooling tower has received little attention. Smrekar et al. [9] showed that by improving the spray arrangement design in the cooling tower, an optimal water distribution with a constant water/air mass flow rate can be achieved which can improve the cooling tower efficiency by 5.5% [9]. The aim of this study is to better understand the use of saline water in spray assisted natural draft cooling towers. The current research focuses on the performance of different nozzle arrangements within a cooling tower. Particularly, how nozzle arrangement affects cooling efficiency and the distance over which saline droplets are not completely evaporated. The proposed model uses the new knowledge obtained from the results of Scanning Electron Microscopy. The model considers the porosity of dried particles with a more realistic way. Finally, a trade-off criteria is presented to help designer to choose the most suitable arrangement.

2. Theoretical Modelling

To simulate the behaviour of the saline water in a spray assisted natural draft dry cooling tower, ANSYS FLUENT release 16.1 is used [10].

2. 1. Governing equations

An Eulerian - Lagrangian approach suggested by Nijdam et al. [11] is used. The standard k- ϵ model with the time-averaged Navier-Stokes equations is utilized in this model. The governing equations of the air flow are presented in [3].

In the discrete phase, the trajectory of the droplets is determined by integrating the forces acting on the particle, which is written in a Lagrangian reference frame [12]:

$$\frac{dV_d}{dt} = F_D + \frac{g(\rho_d - \rho_g)}{\rho_d} + F_{x1} \quad (1)$$

where F_D is the drag per unit droplet mass, given by [12]:

$$F_D = \frac{18\mu}{\rho_d D_d^2} \frac{V_r C_D Re}{24} \quad (2)$$

The drag coefficient, C_D is calculated as:

$$C_D = a_1 + \frac{a_2}{Re} + \frac{a_3}{Re^2}, \quad 0.1 \leq Re \leq 50000 \quad (3)$$

where a_1 , a_2 , and a_3 are constants that apply to smooth spherical droplets (here, $a_1 = 1.222$, $a_2 = 29.1667$, and $a_3 = -3.8889$). A comprehensive procedure to determine these constants is presented in [13].

The momentum, heat and mass transfer between the droplets and ambient gas are explained in [3]. After reaching the vaporization temperature, the following mass transfer equation is also applied to the droplets [12]:

$$N = h_D (y_s - y_\infty), \quad (4)$$

The resulting coupled heat transfer equation is:

$$m_d c_p \frac{dT_d}{dt} = h A_d (T_g - T_d) + \frac{dm_d}{dt} h_{fg}, \quad (5)$$

The rate of evaporation, $\frac{dm_p}{dt}$, is zero before the droplets heat up to reach the wet-bulb temperature.

A first order upwind discretization scheme is used for turbulent kinetic energy and dissipation rate, and second order upwind scheme is chosen for momentum and energy. Moreover, the SIMPLE algorithm with staggered grids is used for velocity and pressure couplings.

2. 2. Discrete Phase Model boundary conditions

The Discrete Phase Model (DPM) in ANSYS FLUENT simulates a multicomponent solution in a spray. It contains multi liquids. However, to study saline water spraying, a solid component has to be introduced to the model. To implement solid particles in sprayed water

and predict the size evolution of saline water droplets in ANSYS FLUENT, the evaporation process of a single saline water droplet should be studied. Here, the physical model of evaporation developed by Sadafi et al. [14, 15] is used. In their four-stage model, when a solid containing droplet is exposed to a warm ambient gas, its temperature reaches to around wet-bulb temperature (first stage in Fig. 2). In the second stage, the isothermal evaporation occurs during which the droplet shrinks until it reaches the critical (saturated) concentration.

Next, in the third stage, solidification starts from the bottom of the droplet and grows from the side until a crust covers the droplet surface. Then, in the fourth stage, evaporation continues from the shrinking wet-core. In this stage, vapour diffuses through the pores of the solid crust until the droplet dries out, leaving a porous salt particle.

When air is entrapped in the pores of a porous particle, it is necessary to consider the porosity as it changes the dried size and mean density of the particle [16]. There are limited information regarding the shape and porosity of such dried crystals of saline water droplets. Therefore, the surfaces of dried droplets (stage 4) were investigated using Scanning Electron Microscopy (SEM). Fig. 3 shows the existence of pores on the surface of a crystal formed during a saline water droplet evaporation. According to the observations in [17], 62% of the pores range between 0.5 μm to 1.5 μm in size.

After processing the images obtained from SEM, the surface porosity of the salt particle was determined. The surface porosity is calculated by dividing the void area (total area of the pores) on the surface by the image area. A MATLAB code was created to process multiple images. Fig. 4 shows how the pore locations were detected. The blue dots in Fig. 4– b show the presence of the pores. 31 images were processed and the average surface porosity of the salt was measured to be 6.95%. The actual porosity of dried salt is larger due to the formation of secondary crystals on the surface (Fig. 3). Secondary crystals form on the surface close to the end of each pore because during evaporation a portion of the liquid from the wet-core, is transferred through the pores, and dries on the surface.

Using this information, NaCl was introduced to the DPM as a component in the sprayed solution (3% by mass). In the multicomponent feature of DPM, besides pure water (96.985%), the entrapped air (0.015%) was defined as the third component in the sprayed solution to consider the measured porosity in the final dried particles.

2. 3. *Geometry of simulation*

To simulate nozzle arrangements in a cooling tower, nozzles were positioned either along a 4 m diameter circle or within the circle as shown in Fig. 5. To avoid any wall effect on the spray flow, a 10 m long cylinder with a diameter of 14 m was chosen as the simulation domain. The nozzles inject in the positive Z (upward) direction. The model includes gravity acting in the negative Z direction.

Five arrangements (Fig. 5) were simulated, each using six full cone nozzles.

The half angle of the nozzles is 40° , the injected fluid is saline water with 3% initial NaCl concentration (by mass) and the DPM in ANSYS FLUENT generates groups of droplets with an initial size of $50\mu\text{m}$ from each nozzle. The temperature of the sprayed water is set to 20°C . The saline water mass flow rate of each spray was 0.02 kg/s .

A smooth mesh with 326460 elements is used. To assess the mesh dependency of the results a spatial convergence examination is performed on the numerical grid using the grid convergence index (GCI) method explained by Roache [18]. The GCI is [19]:

$$GCI = \frac{F_s |\varepsilon|}{r^p - 1} \quad (6)$$

In Eq. (6) F_s is a safety factor numerical value of which is suggested to be 3.0 for comparing results from two different grids [19]. ε and r are the relative error of the solutions and the grid refinement ratio ($r > 1$), respectively. p has a numerical value of two and is the order of convergence. The GCI is determined at the least stable region in the domain, which based on the simulation is downstream of the nozzle. Considering a 0.5 m cylinder with a length of 1 m and grid refinement ratio of 1.33, the maximum GCI is 2.1% among the important variables regarding the nature of the flow. This small value for GCI shows a negligible dependence of the results on the grid size.

3. Numerical Results and Discussion

The validity of the proposed model was previously demonstrated for a single saline water droplet as well as a single nozzle spraying saline water (Fig. 6).

In the current study, the ambient air data for the simulation are based on a hot summer day in Miles, Queensland. According to Australian Government, Bureau of Meteorology [20], we assumed ambient air temperature of 40°C with 44% relative humidity [21]. Within the domain the air velocity was set to 1.5 m/s .

Fig. 7 shows the area mean temperature for concentric circles with width of 1 m and Fig. 8 shows the contour plots of temperature in a horizontal plane 3 m away from the nozzles. This distance was chosen as all saline droplets had evaporated to the 4th stage of the model in [22] by the time they reach this distance. Due to different arrangements of nozzles there are different temperatures in each region.

However, to perform a quantitative comparison between different arrangements, an area weighted mean temperature is considered as:

$$T_{Area\ weighted} = \frac{\sum_{i=n}^m r_i^2 T_i}{\sum_{i=n}^m r_i^2}, \quad (7)$$

where r_i and T_i are the i th terms of radius and temperature.

Using the area weighted mean temperatures, cooling efficiency was defined as:

$$h_{\text{Cooling}} = \frac{T_{\text{inlet}} - T_{\text{outlet}}}{T_{\text{inlet}} - T_{\text{wetbulb}}}, \quad (8)$$

where T_{inlet} and T_{wetbulb} are based on the ambient air upstream of the nozzle and T_{outlet} is based on the mean temperature on a 3 m diameter disc, placed 3 m downstream of the nozzle. This efficiency indicates the performance of the nozzle and sprayed liquid to achieve maximum evaporation 3 m from the nozzle. Table 1 lists the mean temperatures and cooling efficiencies obtained from the simulations as well as the wet lengths.

As shown in Table 1, arrangement 2 has the lowest mean temperature and highest cooling efficiency, while arrangement 3 is the least efficient. Therefore, using the optimum nozzle arrangement may improve the cooling efficiency by 2.05% and may increase mean temperature reduction by 10%. An economic study Ashwood and Bharathan showed that a 7.5 °C reduction in temperature due to spray cooling leads to 14% improvement in power generation rate in a 20 MW power plant [1].

The other important parameter involved in using saline water for spray cooling is wet length. Wet length is the distance from the nozzles for which the air stream is still wet. This length is important as installing the heat exchangers before it leads to corrosion and increases the chance of deposition of salt on the surfaces. Using the four-stage model of [3], the evolution of a single saline water droplet radius follows the trend shown in Fig. 9. During the first and second stages, the droplet surface is wet, while in the third stage the surface of droplet is partially dry. Finally, in the fourth stage, a dry layer of salt covers the liquid droplet, resulting in dry particles and consequently a dry air stream. However evaporation continues as the liquid inside the porous salt particle evaporates.

The percentage of droplets with a wet-surface, as a function of distance from the nozzle plane, is shown in Fig. 10 for the five nozzle arrangements. After the start of the fourth stage (end of wet length), 100% of the droplets are dry. This figure shows that for all arrangements there is little variation in the distance at which stage 4 is reached (less than 0.15 m). Comparing the different arrangements shows that arrangement 5, with the most uniform spacing of nozzles yields the shortest wet length and that arrangements where nozzles are clustered towards the centre of the circle (1 and 4) have a longer wet length.

Different performances for the five arrangements are due to the interaction between adjacent nozzles. In other words, arrangement 2 has the highest cooling efficiency because the spray areas of the nozzles have the least overlap among the five arrangements, leading to most uniform cooling. On the other hand, the cooled area in arrangement 3 is concentrated at the middle of the domain (Fig. 8). Therefore, arrangement 3 is affecting a smaller area which leads to a higher mean temperature and consequently less improved cooling efficiency. The interaction between the nozzles is independent from the ambient conditions (gas temperature, relative humidity, and velocity in the range of natural draft cooling tower operating condition). Thus, these results are applicable for different cooling tower representative ambient conditions. To determine wet length, the last single droplet with numerically wet surface is considered in the model. The location with dry surface for all droplets not only depends on the ambient conditions and geometry, but also is a function of turbulence effects.

Therefore, the arrangement with the best cooling efficiency has not necessarily the shortest wet length. According to the obtained results in the current study and the ones reported in [4], different nozzle arrangements have a weak influence on wet length compared to ambient and initial conditions including: gas temperature, relative humidity, velocity, droplet size, and water mass flow rate. The presence of a dry stream is a complex interaction between the evaporation process, which affects the droplet mass and the droplet falling velocity relative to the free-stream, which is highly dependent on localised fluid flow [23].

As shown in Table 1, the shortest wet length corresponds to arrangement 5, which has a sub-optimal cooling efficiency. Therefore to determine the optimum design a trade-off between this factor and cooling efficiency is required. According to certain circumstances, a designer may choose an arrangement with a low cooling efficiency and low but short wet length, or an improved efficiency, but long wet length.

For the conditions described in this work, cooling efficiency is a stronger design parameter, because the wet lengths are very similar. However, in certain circumstances with different initial conditions, the wet length might be more important. The selection of an arrangement should consider the limitation of the project including: available area and vertical length, budget, ambient conditions, available mass flow of water, etc.

4. Conclusion

The influence of nozzle arrangement on the cooling performance of a spray system using saline water in a natural draft dry cooling tower was investigated. To develop a numerical model allowing usage of solid particles in the sprayed water, porosity and shape of final dried crystals were studied using Scanning Electron Microscopy. After simulating saline water sprays, five different nozzle arrangements each with six nozzles were simulated. It was shown that an efficient nozzle arrangement achieves 2.91% higher cooling efficiency. Moreover, different arrangements of nozzles results in formation of different wet lengths. For all arrangements the formation of a solid crust is achieved over a short distance and full evaporation is achieved before 2.26 m from the nozzles. The nozzle arrangement does not influence the wet length significantly.

Acknowledgments

This research was performed as part of the Australian Solar Thermal Research Initiative (ASTRI), a project supported by the Australian Government, through the Australian Renewable Energy Agency (ARENA).

Nomenclatures

A	surface area (m^2)	t	time (s)
a_1, a_2, a_3	constants in drag coefficient calculation	T	temperature (K)

c_p	specific heat (J/kg K)	V	velocity (m/s)
C_D	drag coefficient	y	molar concentration
D	diameter (m)	ε	relative error of solution
F_D	drag force per unit mass (m/s^2)	η_{Cooling}	cooling efficiency (%)
F_s	safety factor	ρ	density (kg/m^3)
F_{xl}	additional acceleration (m/s^2)	μ	dynamic viscosity (kg/m s)
g	gravitational acceleration (m/s^2)		
GCI	grid convergence index	<i>Subscripts</i>	
h	sensible enthalpy (J/kg)		
h_D	mass transfer coefficient ($\text{kg mol/m}^2 \text{ s}$)	d	droplet
h_{fg}	specific enthalpy of evaporation (J/kg)	g	gas
m	mass (kg)	i	Cartesian component
N	molar flux of vapour ($\text{kg mol/m}^2 \text{ s}$)	<i>inlet</i>	condition at entry of computational cell
p	order of convergence	<i>outlet</i>	condition at exit of computational cell
r	grid refinement ratio	s	surface
R	radius of domain (m)	r	relative
Re	Reynolds number = $\frac{D_d V_r}{\nu_g}$	<i>wetbulb</i>	wet-bulb
RH	relative humidity	∞	free stream

References

- [1] A. Ashwood, D. Bharathan, Hybrid cooling systems for low-temperature geothermal power production, in, National Renewable Energy Laboratory, Golden, CO, 2011, pp. 1-62.
- [2] J.C. Kloppers, D.G. Kröger, Cooling tower performance evaluation: Merkel, Poppe, and e-NTU methods of analysis, Journal of Engineering for Gas Turbines and Power, 127 (2005) 1-7.
- [3] M.H. Sadafi, I. Jahn, K. Hooman, Cooling performance of solid containing water for spray assisted dry cooling towers, Energy Conversion and Management, 91 (2015) 158-167.

- [4] M.H. Sadafi, S.G. Ruiz, M.R. Vetrano, I. Jahn, J.v. Beeck, J.-M. Buchlin, K. Hooman, An investigation on spray cooling using saline water with experimental verification, *Energy Conversion and Management*, 108 (2016) 336-347.
- [5] T. Ohwaki, W. Urushihara, J. Kinugasa, K. Noishiki, Aluminum alloy material having an excellent sea water corrosion resistance and plate heat exchanger, in, Google Patents, 2014.
- [6] G. Kronenberg, F. Lokiec, Low-temperature distillation processes in single- and dual-purpose plants, *Desalination*, 136 (2001) 189-197.
- [7] R. Rao, V. Patel, Optimization of mechanical draft counter flow wet-cooling tower using artificial bee colony algorithm, *Energy Conversion and Management*, 52 (2011) 2611-2622.
- [8] M.P. Galiyano, M.J. Galiyano, B.R. Wiggs, J.T. Aspacher, Modular tube bundle heat exchanger and geothermal heat pump system, in, Google Patents, 1993.
- [9] J. Smrekar, J. Oman, B. Širok, Improving the efficiency of natural draft cooling towers, *Energy Conversion and Management*, 47 (2006) 1086-1100.
- [10] ANSYS FLUENT® Academic Research, Release 16.1, in, 2015.
- [11] J.J. Nijdam, B. Guo, D.F. Fletcher, T.A. Langrish, Lagrangian and Eulerian models for simulating turbulent dispersion and coalescence of droplets within a spray, *Applied mathematical modelling*, 30 (2006) 1196-1211.
- [12] ANSYS FLUENT Theory Guide, 2011.
- [13] S. Morsi, A. Alexander, An investigation of particle trajectories in two-phase flow systems, *Journal of Fluid Mechanics*, 55 (1972) 193-208.
- [14] M.H. Sadafi, I. Jahn, A.B. Stilgoe, K. Hooman, A theoretical model with experimental verification for heat and mass transfer of saline water droplets *International Journal of Heat and Mass Transfer*, 81 (2015) 1-9.
- [15] M.H. Sadafi, I. Jahn, A.B. Stilgoe, K. Hooman, Theoretical and experimental studies on a solid containing water droplet, *International Journal of Heat and Mass Transfer*, 78 (2014) 25-33.
- [16] S. Lowell, J.E. Shields, Powder surface area and porosity, Springer Science & Business Media, 2013.
- [17] M.H. Sadafi, I. Jahn, A.B. Stilgoe, K. Hooman, An investigation of evaporation from single saline water droplets: experimental and theoretical approaches, in: 19th Australasian Fluid Mechanics Conference, Melbourne, VIC, 2014.
- [18] P.J. Roache, *Fundamentals of computational fluid dynamics*(Book), Albuquerque, NM: Hermosa Publishers, 1998., (1998).
- [19] J.W. Slater, Examining spatial (grid) convergence, Public tutorial on CFD verification and validation, NASA Glenn Research Centre, MS, 86 (2006).
- [20] Queensland Government, Department of Energy and Water Supply, in, <https://www.dews.qld.gov.au>, 2014.
- [21] <http://www.bom.gov.au/>, in, 2014.
- [22] M.H. Sadafi, I. Jahn, A.B. Stilgoe, K. Hooman, A theoretical model with experimental verification for heat and mass transfer of saline water droplets, *International Journal of Heat and Mass Transfer*, 81 (2015) 1-9.
- [23] R. Kronig, J.C. Brink, On the theory of extraction from falling droplets, *Applied Scientific Research*, 2 (1951) 142-154.

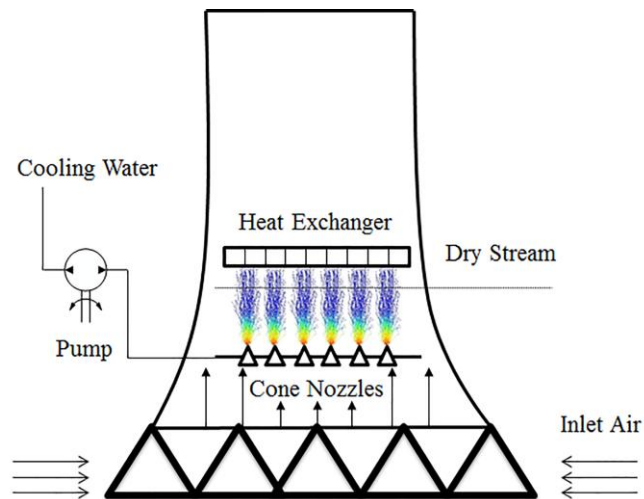


Fig. 1. Dry stream in a spray assisted natural draft dry cooling tower using saline water

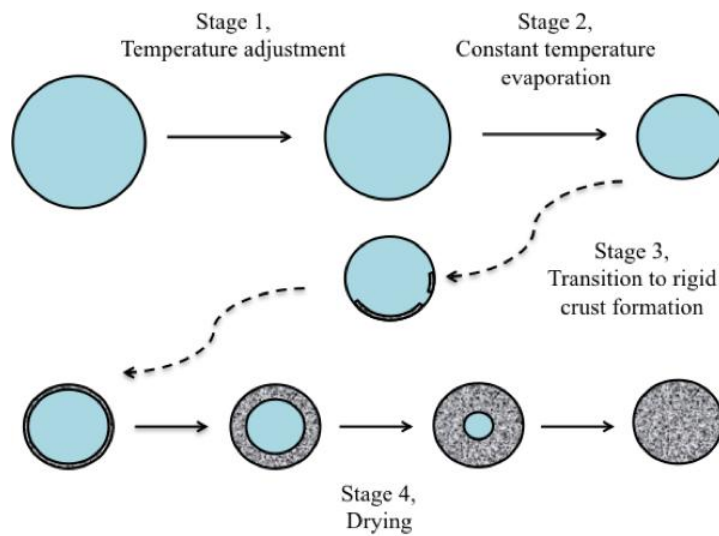


Fig. 2. Evaporation of a solid containing liquid droplet in hot ambient gas

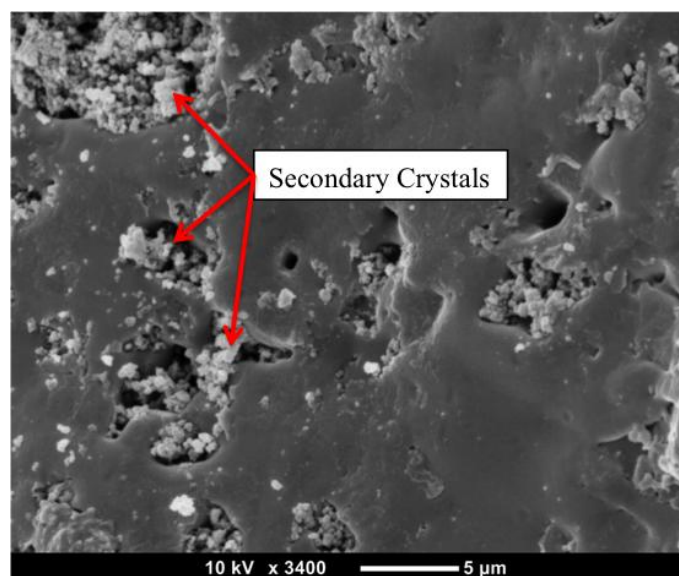


Fig. 3. Scanning Electron Microscopy image of NaCl crystal created from evaporation experiments; formation of secondary crystals

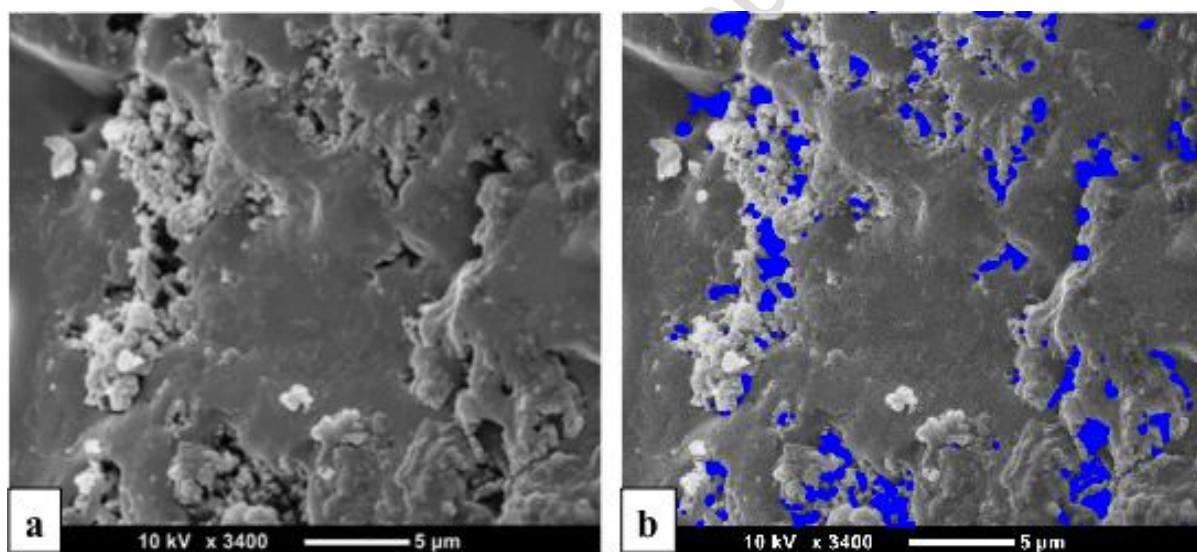


Fig. 4. SEM image before and after image processing; the blue dots locate the pores on the surface.

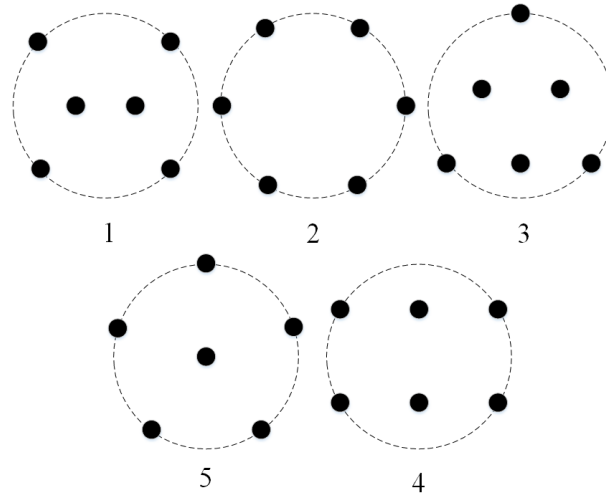


Fig. 5. The studied nozzle arrangements in the domain

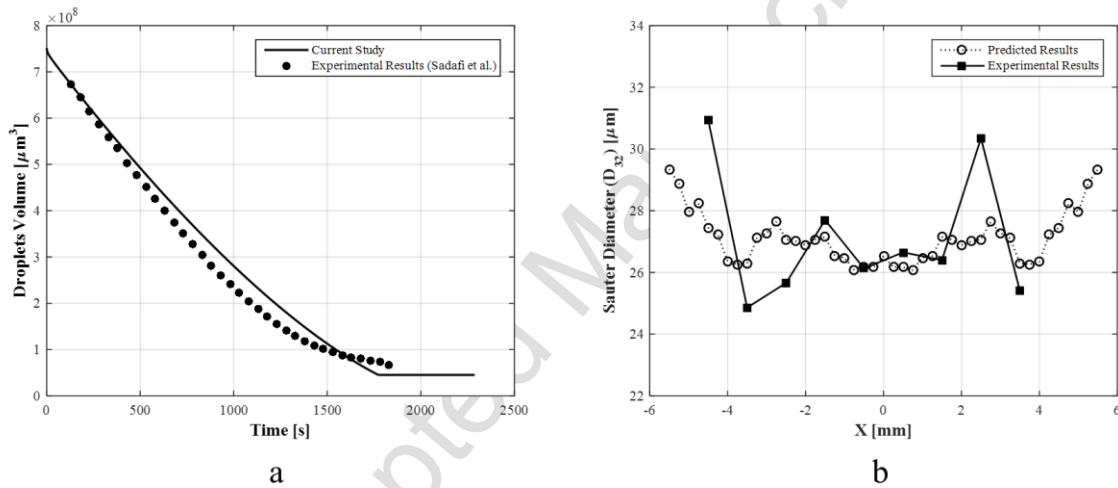


Fig. 6. Validation of the model for (a) volume of single saline water droplet with 3% initial concentration at 24 °C [3], and (b) D_{32} of the spray 5 mm from the nozzle with the half angle of 40° and saline water with 3% initial NaCl concentration at 23 °C and 58% relative humidity [4].

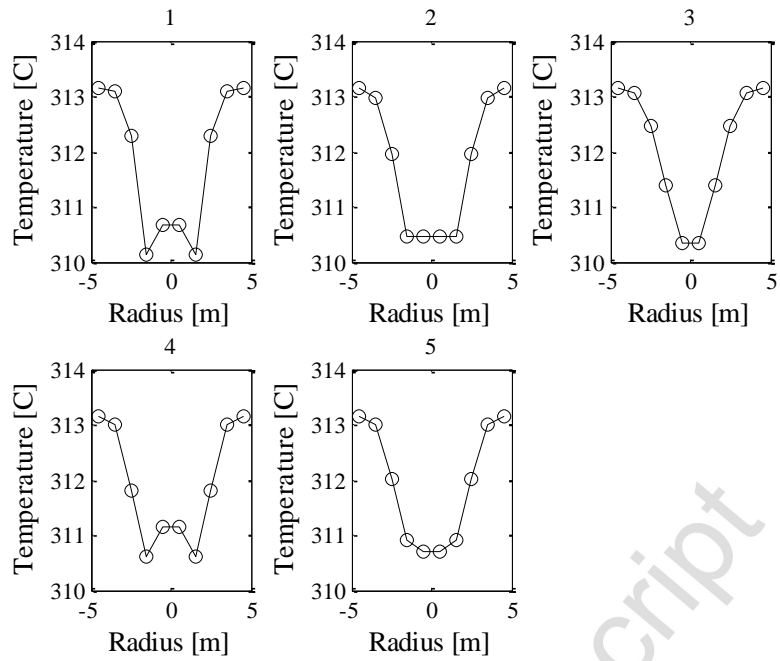


Fig. 7. Area weighted mean temperature change in a perpendicular plane 3 m from the nozzles.

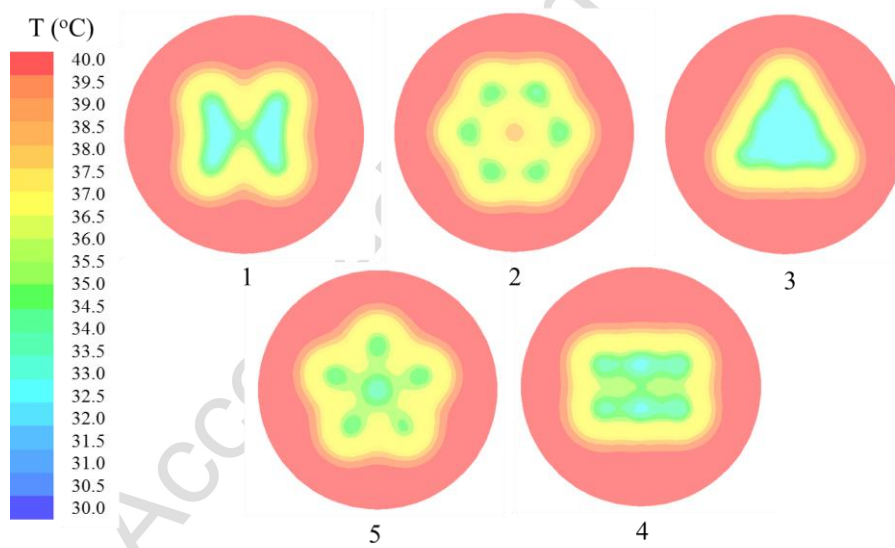


Fig. 8. Temperature contours in a perpendicular plane 3 m from the nozzles.

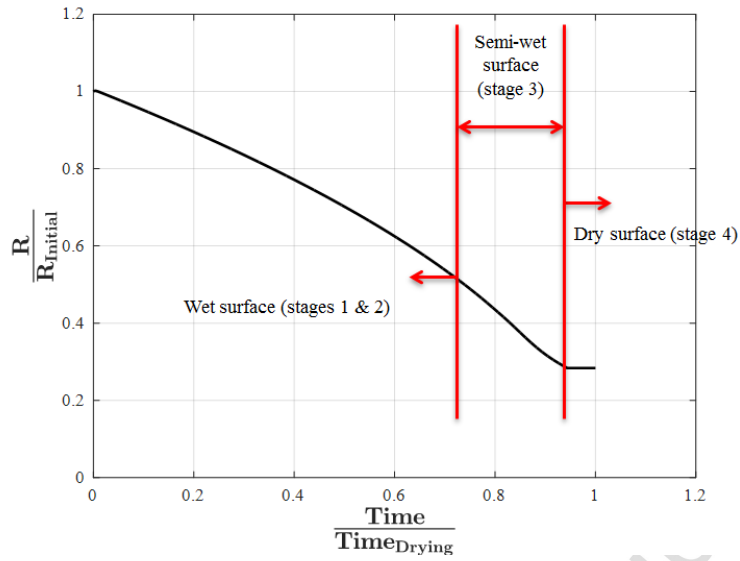


Fig. 9. Numerical results for dimensionless radius of a single saline water droplet against dimensionless time ($T=40\text{ }^{\circ}\text{C}$, $\text{RH} = 44\%$, $R_0 = 50\text{ }\mu\text{m}$, $c_0 = 3\%$ by mass)

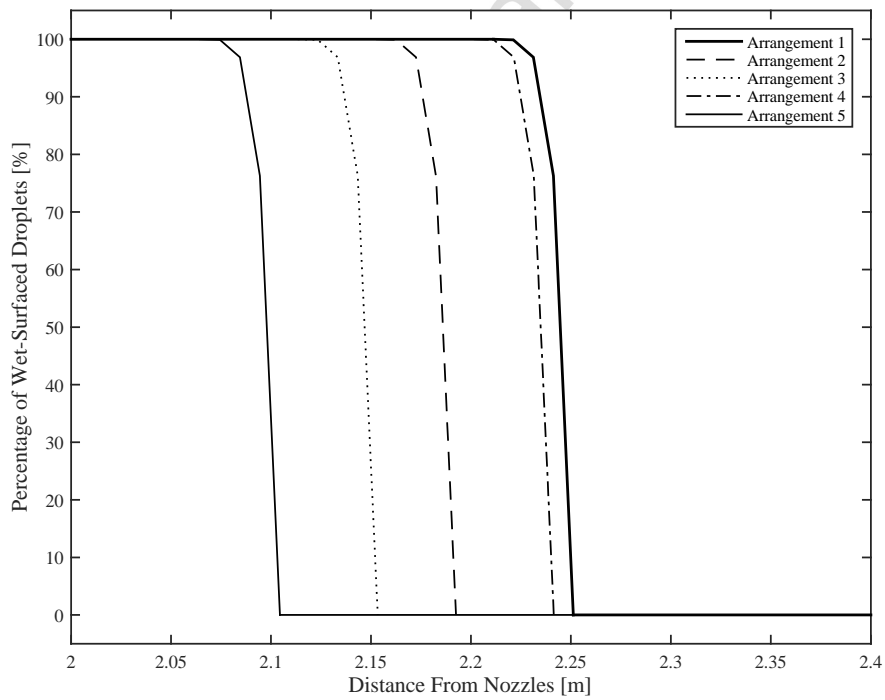


Fig. 10. Percentage of wet-surfaced droplets for different nozzle arrangements shown in Fig. 5

Accepted Manuscript

Table 1 Cooling efficiency and mean temperature of different arrangements

Arrangement No.	Cooling Efficiency [%]	Area Weighted Mean Temperature [°C]	Wet Length (m)
1	20.35	37.76	2.26
2	21.47	37.64	2.20
3	19.42	37.86	2.16
4	20.25	37.77	2.25
5	20.52	37.74	2.11

Accepted Manuscript